

Fine Strontium Ferrite Powders from an Ethanol-Based Microemulsion

Jiye Fang,[†] John Wang,^{*†} Leong-Ming Gan,^{‡,§} Ser-Choon Ng,[¶] Jun Ding,[†] and Xiangyuan Liu[†]

Department of Materials Science, Department of Chemistry, Institute of Materials Research and Engineering, and Department of Physics, Faculty of Science, National University of Singapore, Singapore 119260, Republic of Singapore

A fine strontium ferrite powder with high coercivity was successfully prepared by forming hydroxide precursor particles in the continuous ethanol-based phase of a microemulsion consisting of iso-octane, NP9, and an ethanol solution containing Sr²⁺ and Fe³⁺ cations at a molar ratio of 1:12. The microemulsion-derived hydroxide precursor was calcined at various temperatures, ranging from 600° to 1100°C, to develop the hexagonal strontium ferrite phase. X-ray diffractometry and infrared characterizations revealed that the formation mechanisms of strontium ferrite in the microemulsion-derived precursor differed from those of the precursor derived by conventional coprecipitation. The microemulsion resulted in a strontium ferrite of finer particle size and better magnetic properties than those of the conventionally coprecipitated strontium ferrite. The microemulsion-derived strontium ferrite exhibited an intrinsic coercivity of 6195 Oe and a saturation magnetization of 58.28 emu/g when calcined at 900°C. The saturation magnetization increased further, to 69.75 emu/g, when the microemulsion-derived precursor was calcined at 1100°C.

I. Introduction

STRONTIUM HEXAFERRITE, SrFe₁₂O₁₉, is a ferrimagnet in which iron ions in five different crystallographic sites are coupled antiferromagnetically. This ferrimagnet exhibits a high saturation magnetization and high coercivity because of the relatively high magnetocrystalline anisotropy field.¹ SrFe₁₂O₁₉ has been explored for many technologically demanding and challenging applications, such as for permanent magnets¹ and high-density perpendicular recording media, with proper doping.² The properties of strontium ferrite are largely dependent on the processing routes used for fabrication, as reviewed by Stäblein³ and Kojima.⁴ Traditionally, SrFe₁₂O₁₉ powders have been synthesized by the solid-state reaction between SrCO₃ and Fe₂O₃ at a high calcination temperature (~1300°C).⁵ However, this technique apparently is associated with disadvantages, such as large particle and agglomerate sizes and uncontrolled particle morphology. The subsequent milling of the calcined strontium ferrite powders undoubtedly introduces a level of contamination and, therefore, degrades the magnetic properties.⁶

Multidomain ferrites, including SrFe₁₂O₁₉, increase in coercivity as particle size decreases.⁷ Therefore, the preparation of a strontium ferrite powder with refined particle size, narrowed

particle-size distribution, and minimal particle agglomeration has received considerable attention.⁸ Numerous novel processing routes have been devised, including coprecipitation,^{9–12} hydrolysis of metallorganic complexes,¹³ sol–gel synthesis,^{14–16} spray pyrolysis,¹⁷ the citrates method,^{2,14,16} glass-crystallization,^{18–21} and hydrothermal reaction.^{22–24} Ultrafine SrFe₁₂O₁₉ powders with particle sizes in the range of ~50 nm have been prepared successfully via some of these processing routes, but the magnetic properties of the resulting ferrite powders vary considerably from one material to another. For example, Choy *et al.*¹⁴ reported a coercive force of 6500 Oe (1 Oe = 80 A/m) for one of the strontium ferrite powders prepared via a sol–gel processing route, although the powder exhibits a relatively low saturation magnetization (50 emu/g).

One of the major difficulties encountered in many of these wet-chemistry-based processing routes for strontium ferrites, such as coprecipitation¹⁰ and hydrothermal reaction,²⁵ is the relatively high solubility of Sr(OH)₂ in an aqueous solution. This solubility poses problems in maintaining the stoichiometry of the strontium ferrite, although excess strontium can be introduced into the starting composition. For example, a Sr²⁺:Fe³⁺ ratio as high as 1:8 was used by Ataie *et al.*²⁵ in their hydrothermal solution, and a Sr²⁺:Fe³⁺ ratio of 1:11 was used by Kulkarni *et al.*¹⁰ in their coprecipitation route, in comparison with the stoichiometric ratio of 1:12 in SrFe₁₂O₁₉. To reduce the solubility of Sr(OH)₂, various measures, such as raising the [OH⁻]/[NO₃⁻] molar ratio in the aqueous solution, have been adopted in some processing routes.^{23,25} This method is related to the fact that strontium hydroxide is alkaline, because a strong alkaline environment favors Sr(OH)₂ precipitates.

Synthesis of ultrafine ceramic powder particles in the aqueous droplets of both inverse and bicontinuous microemulsions has been reported elsewhere.^{26–29} However, for strontium ferrite, the inverse water-in-oil microemulsions may not be ideal, because of the high solubility of strontium hydroxide, although the inverse microemulsion domains may be able to produce a nanosized precursor particle. The objectives of the present work are (i) to study the feasibility of synthesizing a fine strontium ferrite powder in the continuous ethanol-based phase of a microemulsion and (ii) to investigate the relationships between magnetic properties and powder characteristics of the microemulsion-derived strontium ferrite powder, in comparison with those of the materials prepared via conventional coprecipitation.

II. Experimental Procedure

(1) Starting Materials

The starting materials used in the present work included ferric nitrate hexahydrate (>99.4%, Fisher Scientific Co., Pittsburgh, PA), strontium chloride hexahydrate (99.995%, Aldrich Chemical Co., Milwaukee, WI), tetramethylammonium hydroxide solution (~1.1M, Fluka Chemical AG, Buchs, Switzerland), a high-purity ethanol (>99.5 vol%, CSR Chemicals, Victoria, Australia), iso-octane (assayed by gas chromatography as 100%, J. T. Baker Chemical, Phillipsburg, NJ), a nonionic surfactant of polyoxyethylene(9) nonylphenol ether (NP9, Albright & Wilson Asia Pacific Pte. Ltd., Singapore).

L. Levinson—contributing editor

Manuscript No. 189522. Received March 1, 1999; approved October 5, 1999. Supported by the National University of Singapore, under Research Grant No. RP3979900, and the Institute of Materials Research and Engineering (IMRE), under Research Grant No. GR6611.

*Member, American Ceramic Society.

[†]Department of Materials Science.

[‡]Department of Chemistry.

[§]Institute of Materials Research & Engineering.

[¶]Department of Physics.

(2) Phase Diagrams

The procedure used for establishing a partial phase diagram at room temperature for the ternary system consisting of iso-octane, NP9, and ethanol was similar to those detailed elsewhere.^{26,30} To locate the demarcation between the microemulsion and the non-microemulsion regions, the alcohol solution containing ferric nitrate ($\text{Fe}(\text{NO}_3)_3$) and strontium chloride (SrCl_2) was titrated into a mixture of a given iso-octane:NP9 ratio. Thorough mixing of the three components was achieved using a Vortex mixer, which generated a high frequency of shaker mixing at room temperature. The microemulsion of fine iso-octane droplets dispersed in the continuous ethanol phase appeared optically transparent. A series of such demarcation points was obtained by varying the iso-octane:surfactant ratio. Partial phase diagrams, at room temperature, were established for two ternary systems, consisting of iso-octane, NP9, and a polar ethanol phase containing either $0.02M \text{SrCl}_2 + 0.24M \text{Fe}(\text{NO}_3)_3$ or $0.50M (\text{CH}_3)_4\text{N}(\text{OH}) + 25.2M \text{H}_2\text{O}$.

(3) Preparation of $\text{SrFe}_{12}\text{O}_{19}$ Precursor

Two microemulsion compositions, both consisting of 15.0 wt% iso-octane, 15.0 wt% NP9, and 70.0 wt% ethanol containing either $0.02M \text{SrCl}_2 + 0.24M \text{Fe}(\text{NO}_3)_3$ or $0.50M (\text{CH}_3)_4\text{N}(\text{OH}) + 25.2M \text{H}_2\text{O}$, were prepared. The coprecipitation reaction was effected when the composition containing SrCl_2 and $\text{Fe}(\text{NO}_3)_3$ was titrated into the composition containing $(\text{CH}_3)_4\text{N}(\text{OH})$ in a volume ratio of 1:2 at room temperature. The precipitates then were retrieved and washed repeatedly, using a mixed solvent consisting of acetone and ethanol in a 1:2M ratio. The precursor was subsequently dried in a vacuum oven, first at 60°C and then at 90°C , for 12 h. Figure 1 is a flow chart showing the steps involved in preparing $\text{SrFe}_{12}\text{O}_{19}$ powders via the ethanol-based microemulsion route.

For comparison, hydroxide precursors of strontium ferrite also were prepared via a conventional coprecipitation route. For this procedure, 100 mL of ethanol solution containing $0.02M \text{SrCl}_2 + 0.24M \text{Fe}(\text{NO}_3)_3$ was added dropwise into 200 mL of ethanol solution containing $0.50M (\text{CH}_3)_4\text{N}(\text{OH}) + 25.2M \text{H}_2\text{O}$, with vigorous stirring. The resulting precipitates were recovered and dried by following the steps detailed above for the microemulsion route.

(4) Powder Characterization

The as-dried precursor powders from the above two routes were characterized by thermogravimetric analysis (TGA; Model No. 2950, DuPont/Clinical and Instrument Systems Division, Wilmington, DE) and differential thermal analysis (DTA; Model No. 1600, DuPont), with Al_2O_3 as the reference, at a heating rate of $10^\circ\text{C}/\text{min}$, in air, from room temperature to 950°C . The powders

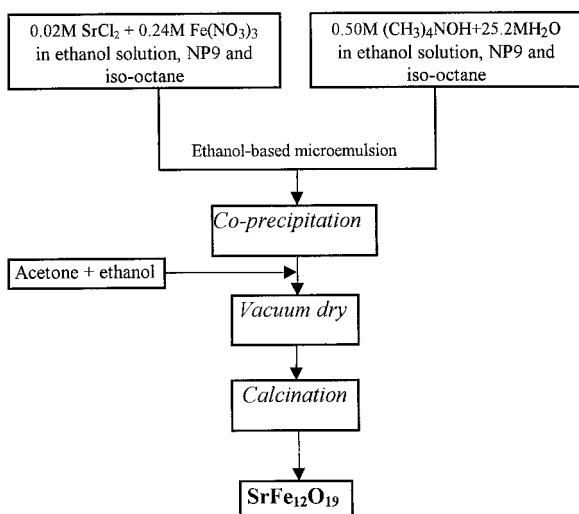


Fig. 1. Flow chart for preparing $\text{SrFe}_{12}\text{O}_{19}$ powders via the ethanol-based microemulsion route.

then were calcined in air at various temperatures, up to 1100°C , and analyzed using a Fourier transform infrared (FTIR) spectrometer (Model No. FTS135, Bio-Rad Laboratories, Cambridge, MA) over the spectrum range $4000\text{--}400 \text{ cm}^{-1}$. Phase identification in the calcined strontium ferrite powders was conducted at room temperature, using X-ray diffractometry (XRD; $\text{CuK}\alpha$, Model No. PW1729, Philips Analytical X-Ray, Almelo, The Netherlands) and Mössbauer spectrometry (Model No. LC-9A, Austin Science Associates, Inc., Austin, TX). Brunauer-Emmett-Teller (BET) specific surface-area analysis (Model No. Nova 2000, Quantachrome Corp., Boynton Beach, FL) and transmission electron microscopy (TEM; Model No. 100CX, JEOL, Tokyo, Japan) were used to analyze the specific surface area and particle/agglomerate morphology, respectively, of these powders. Vibrating sample magnetometry (Model No. 9T VSM, Oxford Instruments, Inc., Concord, MA) was used to characterize the magnetic properties of the powders, such as intrinsic coercivity and saturation magnetization at room temperature (maximum applied field, $H_{\text{max}} = 6 \text{ T}$).

III. Results and Discussion

(1) Phase Diagrams and Thermal Analysis

Figure 2(a) shows the partial phase diagram established at room temperature for the ternary system consisting of iso-octane, NP9, and the ethanol solution containing $0.02M \text{SrCl}_2 + 0.24M \text{Fe}(\text{NO}_3)_3$. The partial phase diagram for the system containing $0.50M (\text{CH}_3)_4\text{N}(\text{OH}) + 25.2M \text{H}_2\text{O}$ is shown in Fig. 2(b). The shaded areas in both systems represent optically transparent regions, which are nonaqueous microemulsions.^{31,32} Point \oplus , corresponding to the composition of 15.0 wt% iso-octane, 15.0 wt% NP9, and 70.0 wt% ethanol in both systems selected for the preparation of strontium ferrite, is located within the optically

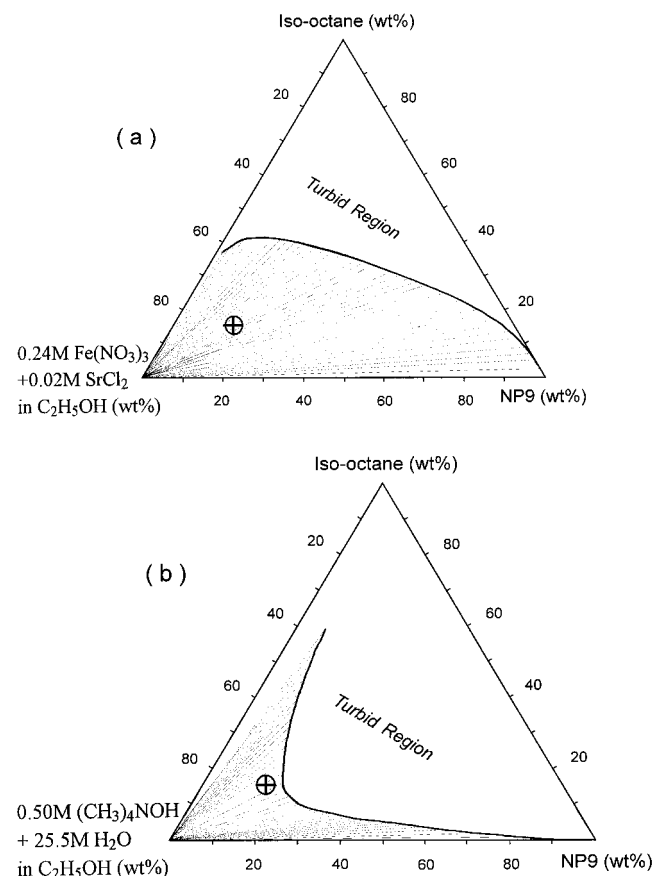


Fig. 2. Partial phase diagram established at room temperature for the ternary systems consisting of iso-octane, NP9, and an ethanol solution containing (a) $0.24M \text{Fe}(\text{NO}_3)_3 + 0.02M \text{SrCl}_2$ and (b) $0.50M (\text{CH}_3)_4\text{NOH} + 25.2M \text{H}_2\text{O}$. Shaded areas represent the transparent microemulsion regions.

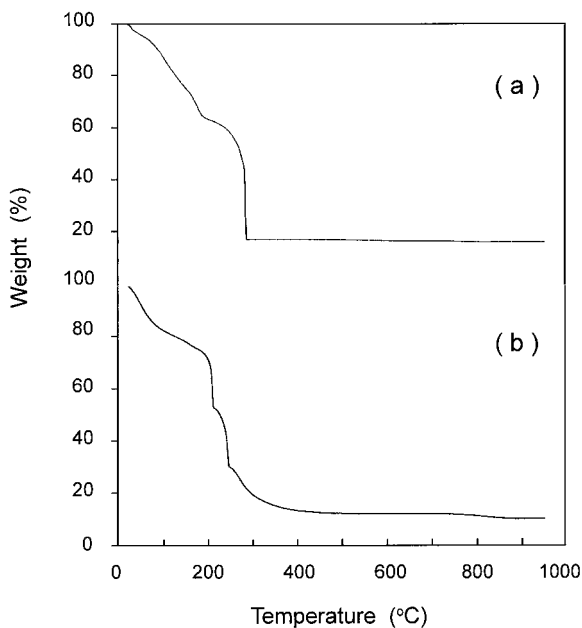


Fig. 3. TGA traces at a heating rate of 10°C/min, in air, for the precursors derived (a) by conventional coprecipitation and (b) from the ethanol-based microemulsion.

transparent region. Conductivity measurement indicated that both compositions are iso-octane-in-ethanol microemulsions.

TGA results for the precursors derived by conventional coprecipitation and from the ethanol-based microemulsion are shown in Figs. 3(a) and (b), respectively; DTA results are shown in Figs. 4(a) and (b), respectively. The conventionally coprecipitated precursor shows two major decreases in specimen weight at temperatures <300°C. The slow, lesser decrease, over the temperature range from room temperature to 180°C, results from the elimination of residual water and solvents, whereas the sharp decrease at ~280°C corresponds to decomposition of the hydroxide precursor. The well-established exothermic peak over the same temperature range indicates a crystallization reaction as soon as the hydroxide precursor has decomposed. The microemulsion-derived precursors

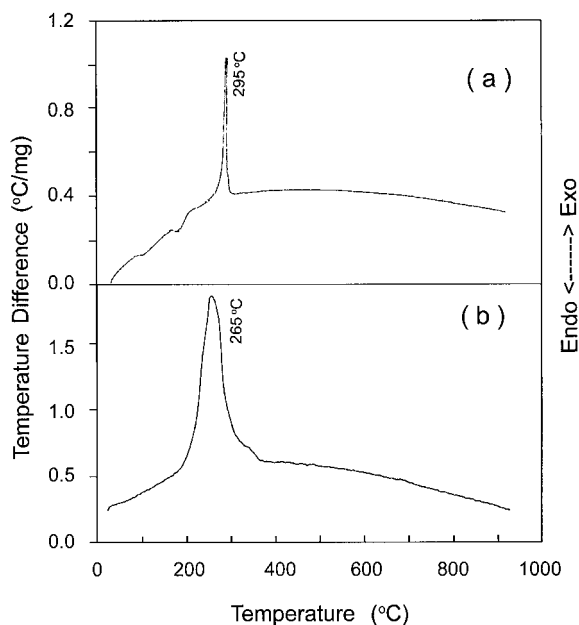


Fig. 4. DTA traces at a heating rate of 10°C/min, in air, for the precursors derived (a) by conventional coprecipitation and (b) from the ethanol-based microemulsion.

exhibit a steady weight loss over the range from room temperature to ~80°C, a result of the evaporation of residual solvent from the as-dried precursors. Three consequential decreases in specimen weight occur over the temperature range 200°–270°C, apparently related to decomposition of the hydroxide precursor into oxide(s), together with the further elimination of organic residuals. This hypothesis is supported by the strong and rather broadened exothermic peak in the DTA trace over the same temperature range. The weight loss continues, with further increases in temperature, to 360°C, after which little further weight loss is observed. Again, the large exothermic peak results from a crystallization reaction, following the decomposition of the hydroxide precursor at a temperature >200°C. Therefore, the process is very similar to those in many other precipitated hydroxide precursors.

(2) Phase Development

To monitor phase development with increasing calcination temperature, the as-dried precursors derived both by conventional coprecipitation and from the microemulsion composition were calcined for 3 h in air at various temperatures, up to 1000°C, then phase analyzed, using XRD at room temperature. Figure 5 illustrates the XRD patterns of the SrFe₁₂O₁₉ precursor derived from the ethanol-based microemulsion calcined for 3 h at various temperatures. Heating the precursor at a rate of 5°C/min to 600°C resulted in a well-crystallized γ -Fe₂O₃ phase^{††} that has been observed as an intermediate phase before formation of the crystalline ferrite in other chemistry-derived precursors.^{13,14} The pattern shows a clear sign of the SrFe₁₂O₁₉ phase, as indicated by the appearance of (107) and (114) peaks at 2 θ angles of 32.37° and 34.25°, respectively, in the powder calcined at 650°C for 3 h.

The amount of SrFe₁₂O₁₉ phase increases as the calcination temperature increases, although an unidentified peak appears at the 2 θ angle of ~31.69°, corresponding to an intermediate phase of either Sr₂FeO₄^{‡‡} or Sr₂Fe₂O₅^{§§} when the powder is calcined at 800°C. At 900°C, SrFe₁₂O₁₉ is the only XRD-detectable phase. As a confirmation of the phase purity, Fig. 6 shows the ⁵⁷Fe

^{††}Powder Diffraction File, Card No. 39-1346. International Centre for Diffraction Data, Newtown Square, PA.

^{‡‡}Powder Diffraction File, Card No. 42-0480.

^{§§}Powder Diffraction File, Card No. 33-0677.

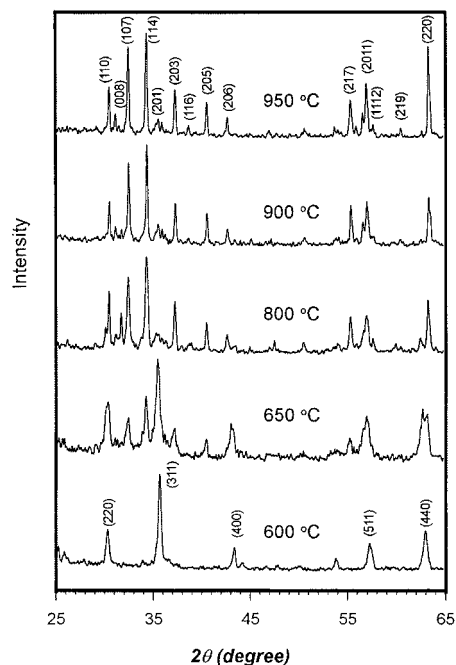


Fig. 5. XRD traces of the powders derived from the ethanol-based microemulsion and calcined for 3 h at various temperatures.

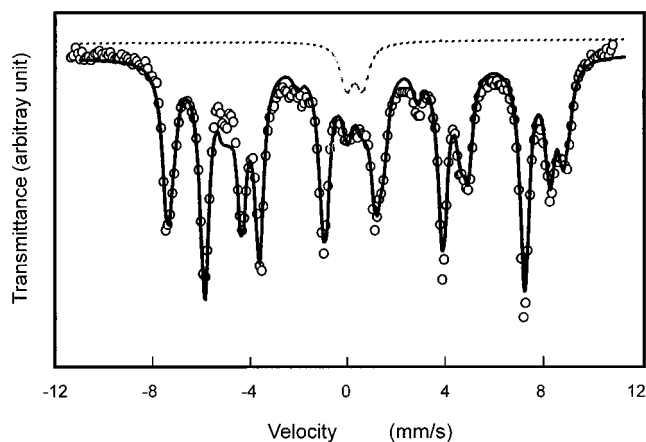


Fig. 6. Mössbauer spectrum, at room temperature, for the microemulsion-derived $\text{SrFe}_{12}\text{O}_{19}$ powder calcined at 900°C for 3 h (○) experimental observation, (—) total fitting curve, and (---) paramagnetic phase).

Mössbauer spectrum for the powder calcined for 3 h at 900°C . This spectrum fits reasonably well with the spectrum of the $\text{SrFe}_{12}\text{O}_{19}$ phase, although a minor amount of paramagnetic phase is present. The formation temperature for $\text{SrFe}_{12}\text{O}_{19}$ in the microemulsion-derived precursors apparently is lower than those observed in the conventional solid-state reaction ($\sim 1300^\circ\text{C}$)⁵ and in the precursors obtained via spray pyrolysis ($\sim 1200^\circ\text{C}$), for forming a single phase of $\text{SrFe}_{12}\text{O}_{19}$.¹⁷ The formation temperature compares reasonably well with those for $\text{SrFe}_{12}\text{O}_{19}$ in the precursors prepared via many other chemistry-based processing routes.^{10,14} The crystallinity of the $\text{SrFe}_{12}\text{O}_{19}$ phase is further enhanced when the calcination temperature is increased to 950°C . As shown in Fig. 7, a mixture of poorly crystallized iron oxide phases is observed at calcination temperatures $< 650^\circ\text{C}$, for the conventionally coprecipitated powder, although a single phase of $\text{SrFe}_{12}\text{O}_{19}$ develops at a high enough calcination temperature.

Figures 8 and 9 are the FTIR spectra for the as-dried precursors derived from the ethanol-based microemulsion and by coprecipitation, respectively, together with spectra for powders calcined at

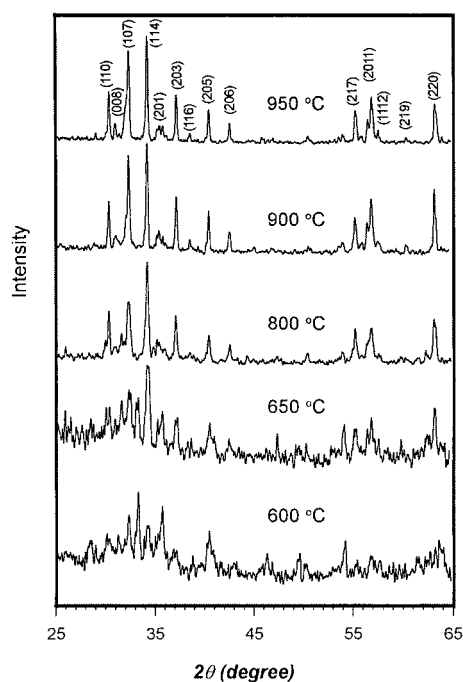


Fig. 7. XRD traces of the powders derived by conventional coprecipitation and calcined for 3 h at various temperatures.

various temperatures. The sharp absorption bands at 946 , 1384 , and 1485 cm^{-1} , and the broad absorption band centered at $\sim 2920\text{ cm}^{-1}$, are from $(\text{CH}_3)_4\text{N}(\text{OH})$;³³ those at 1105 , 1186 , 1249 , 1354 , 1456 , and 1512 cm^{-1} are related to the surfactant residuals in the microemulsion-derived precursor.^{33–35} The bands in the range 438 – 828 cm^{-1} correspond to inorganic groups in both types of precursors.

In Fig. 8, the strong and broadened absorption band at $\sim 3440\text{ cm}^{-1}$ is assigned to vibration of the O–H bond.^{33,35} The intensity of this band decreases when the precursor is heated to 600°C and vanishes completely when it is heated to 900°C . Most of the absorption bands that belong to the organic functional groups of surfactant residuals are eliminated at 600°C . At the same time, three sharp, strong bands at ~ 694 , 858 , and 1456 cm^{-1} are observed as the calcination temperature increases. The bands at ~ 694 and 858 cm^{-1} are attributed to SrCO_3 ,³⁶ which seems to be a transitional phase before the formation of strontium ferrite. The band at 1456 cm^{-1} corresponds to maghemite ($\gamma\text{-Fe}_2\text{O}_3$), confirmed by XRD phase analysis. A comparison of the spectra in Fig. 9 with those in Fig. 8 indicates that SrCO_3 also occurs in the coprecipitated precursor with increasing calcination temperature, as characterized by the band at 858 cm^{-1} . The involvement of hematite ($\alpha\text{-Fe}_2\text{O}_3$), rather than $\gamma\text{-Fe}_2\text{O}_3$, is indicated by the absorption bands at 520 – 600 cm^{-1} and 1350 cm^{-1} .³⁶ Well-established absorption bands at 438 , 549 , and 598 cm^{-1} in the powders calcined at $\geq 900^\circ\text{C}$ indicate the formation of strontium ferrite. Meanwhile, the characteristic bands of SrCO_3 and iron oxides vanish with increasing calcination temperature. This result agrees with the XRD phase-analysis findings.

(3) Particle Characteristics

To show the particle size as a function of calcination temperature, Fig. 10 illustrates the specific surface areas (BET), as a

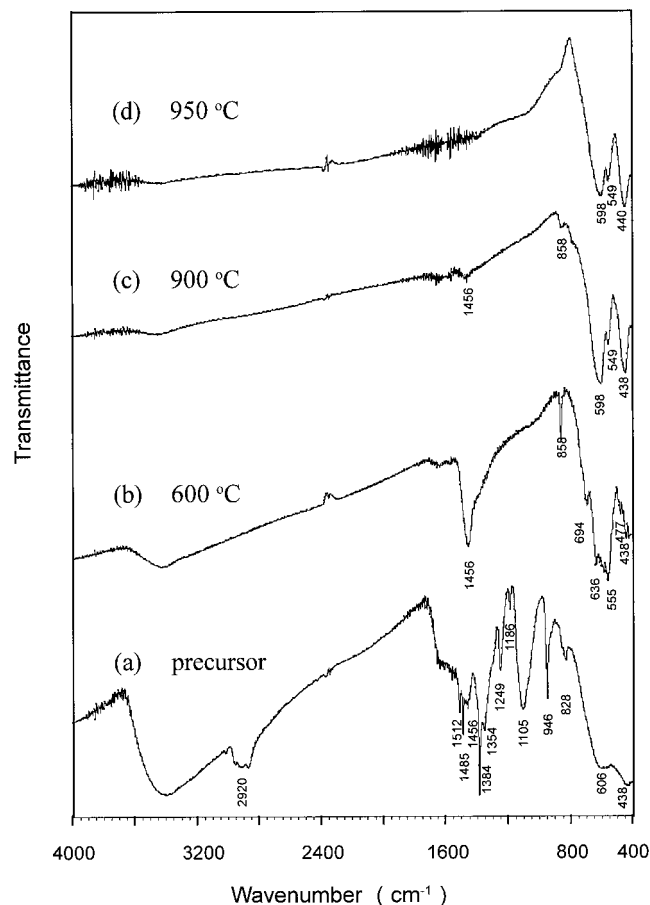


Fig. 8. FTIR spectra of the as-dried precursor derived from the ethanol-based microemulsion and of powders calcined at various temperatures.

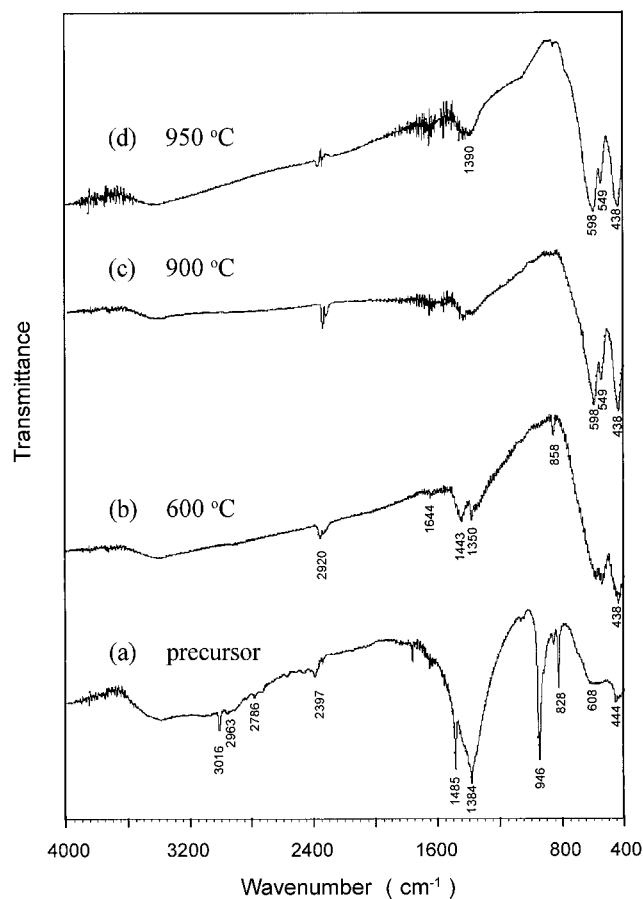


Fig. 9. FTIR spectra of the as-dried precursor derived by conventional coprecipitation and of powders calcined at various temperatures.

function of calcination temperature, over the range 700°–1000°C for the two powders. The specific surface area of the coprecipitated powder is smaller than that of the microemulsion-derived material at each temperature, although both powders show a similar decrease as calcination temperature increases. At 900°C, specific surface areas of 14.90 and 3.64 m²/g were measured for the microemulsion-derived and the conventionally coprecipitated SrFe₁₂O₁₉ powders, respectively. These values correspond to average particle sizes of 78 and 323 nm, respectively, for the two powders.

Figures 11(a,c) and (b,d) are SEM photographs of the two SrFe₁₂O₁₉ powders, derived by conventional coprecipitation and from the ethanol-based microemulsion, respectively. The degree of particle agglomeration in the conventionally coprecipitated SrFe₁₂O₁₉ powder is much higher than in the emulsion-derived powder. The conventionally coprecipitated SrFe₁₂O₁₉ powder is characterized by irregularly shaped particle agglomerates measuring ~60 μm, in contrast to the much smaller particle agglomerates in the emulsion-derived powder. The conventionally coprecipitated SrFe₁₂O₁₉ powder consists of thin plates >1 μm thick, with a large aspect ratio. In comparison, the SrFe₁₂O₁₉ particles derived from the ethanol-based microemulsion have much smaller aspect ratios than those of the conventionally coprecipitated particles, together with much smaller discrete particle sizes.

(4) Magnetic Properties

Figure 12(a) illustrates the saturation magnetization (M_s) of the two SrFe₁₂O₁₉ powders, derived from the ethanol-based microemulsion and by conventional coprecipitation, respectively, as a function of calcination temperature from 650° to 1100°C. The saturation magnetization of the microemulsion-derived strontium

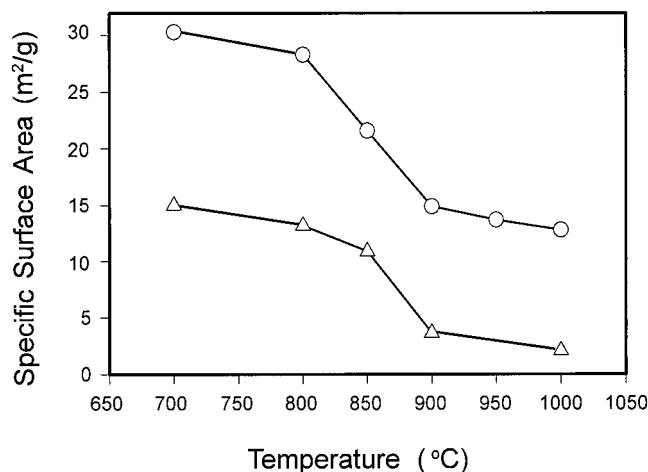


Fig. 10. Specific surface area as a function of calcination temperature ((●) powder derived from the ethanol-based microemulsion and (▲) powder derived by conventional coprecipitation).

ferrite demonstrates an initial decrease when the calcination temperature is increased from 650° to 700°C, followed by a steady increase as the calcination temperature increases within the range 700°–1100°C. The M_s value of 69.75 emu/g obtained for the powder calcined at 1100°C, which is very close to the theoretical M_s value of 74.3 emu/g for strontium ferrite single crystal,¹³ is among the highest values ever reported for SrFe₁₂O₁₉.^{13,22,37} The initial high value of M_s observed for the powder calcined at 650°C accounts for the occurrence of the γ -Fe₂O₃ phase at the intermediate calcination temperature.³⁸ The presence of γ -Fe₂O₃ is confirmed by XRD phase analysis. As the calcination temperature increases from 650° to 800°C, the γ -Fe₂O₃ phase disappears, and a strontium ferrite phase develops. Any further increase in the calcination temperature causes increased crystallinity and particle coarsening of the SrFe₁₂O₁₉. In contrast, the conventionally coprecipitated strontium ferrite exhibits a lower saturation magnetization than that of the microemulsion-derived strontium ferrite at each temperature, although it demonstrates a similar initial decrease, followed by a recovery, with temperature increase.

Figure 12(b) shows the intrinsic coercivity, iH_c , of the two SrFe₁₂O₁₉ powders, as a function of calcination temperature, in the range 650°–1100°C. The microemulsion-derived powder exhibits an almost linear increase in intrinsic coercivity as the calcination temperature increases in the range 650°–900°C. A further increase in the calcination temperature, from 900° to 1100°C, leads to a decrease in intrinsic coercivity. However, the value remains higher than that of the conventionally coprecipitated powder at each calcination temperature. The maximum iH_c value of 6195 Oe obtained at 900°C for the microemulsion-derived ferrite is comparable to the highest values previously reported for fine strontium ferrite powders prepared via many other wet-chemical routes.^{13,14,37,39}

As already established, the intrinsic coercivity of ferrites is strongly affected by their particle/grain sizes.^{7,40} At temperatures <900°C, the dominant factor for improving intrinsic coercivity with increasing calcination temperature is the development of the SrFe₁₂O₁₉ phase, as supported by the XRD phase-analysis results shown in Fig. 5. Nevertheless, enough growth in particle size at too high a temperature results in transition from a single-domain to a multidomain structure. This transition accounts for the decreasing intrinsic coercivity with increasing calcination temperature at >900°C. Correlating the variation in intrinsic coercivity with calcination temperature and the dependence of specific surface area on calcination temperature (Fig. 10) shows that the maximum coercivity occurs at a specific surface area of 14.90 m²/g, corresponding to an average particle size of ~65 nm, which is close to the previously reported values for the critical particle size. A

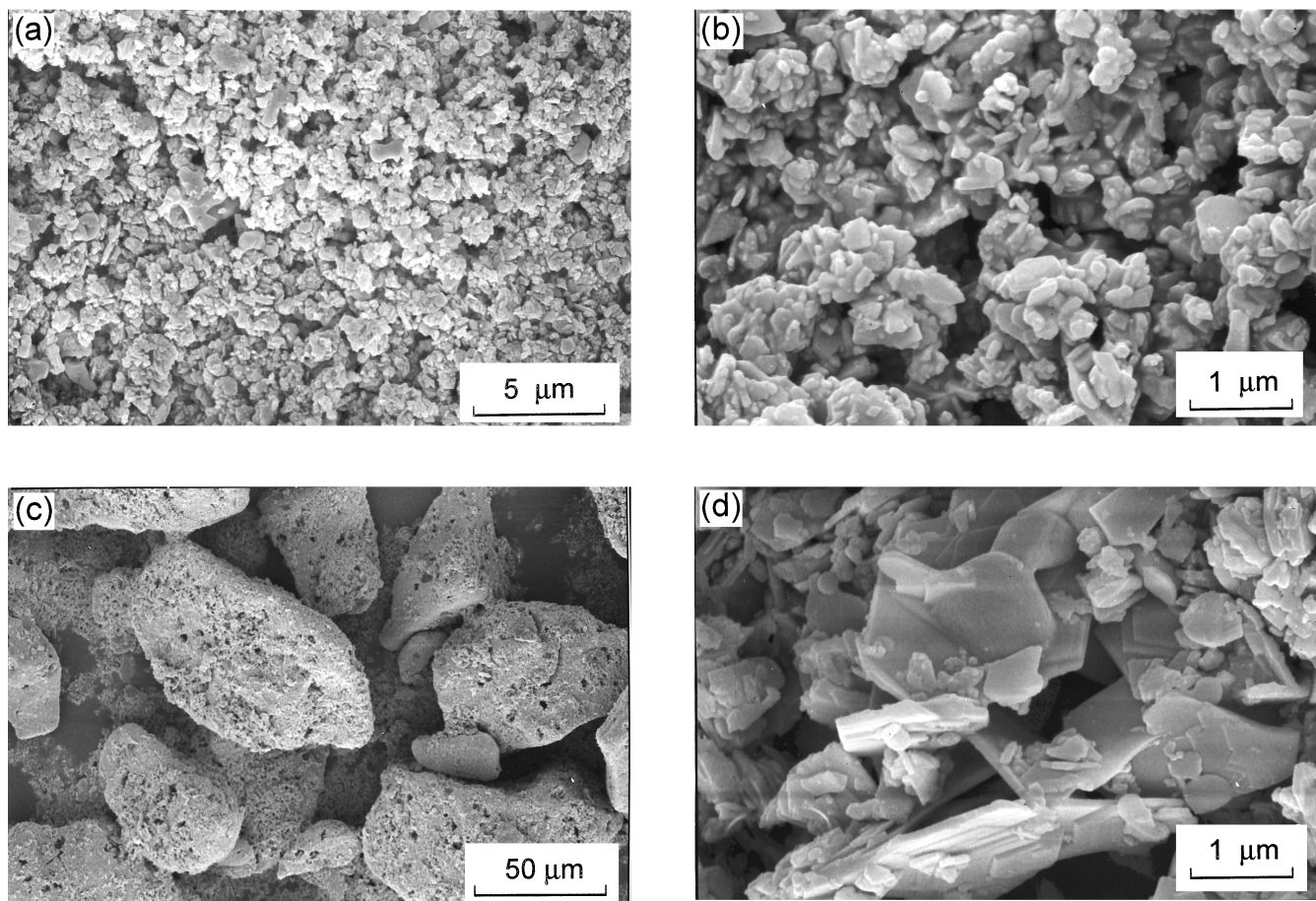


Fig. 11. SEM photographs for the powders derived (a) and (c) by conventional coprecipitation and (b) and (d) from the ethanol-based microemulsion. Both powders were calcined at 900°C for 3 h.

critical size in the range 40–60 nm^{13,14,39} has been suggested for achieving maximum coercivity in SrFe₁₂O₁₉.

IV. Conclusions

A fine strontium ferrite powder with high coercivity was successfully prepared by forming hydroxide precursor particles in an ethanol-based microemulsion consisting of iso-octane, NP9, and an ethanol solution. The coprecipitation reaction was effected by mixing a microemulsion containing Fe(NO₃)₃ and SrCl₂ in the ethanol phase with one containing (CH₃)₄N(OH). A single phase

of SrFe₁₂O₁₉ formed after the precursor was calcined at >900°C. As the calcination temperature was increased, transitional γ-Fe₂O₃ and SrCO₃ phases developed, before the formation of SrFe₁₂O₁₉. The microemulsion-derived SrFe₁₂O₁₉ powder exhibited a much smaller particle size (50–80 nm) than that of the conventionally coprecipitated powder, which was platelike in morphology, with a large aspect ratio. The microemulsion-derived SrFe₁₂O₁₉ powder also demonstrated improved magnetic properties—i.e., saturation magnetization and intrinsic coercivity—over those of the powder derived by conventional coprecipitation. A maximum *iH_c* value of 6195 Oe and an *M_s* value of 58.28 emu/g were obtained for the microemulsion-derived SrFe₁₂O₁₉ calcined at 900°C.

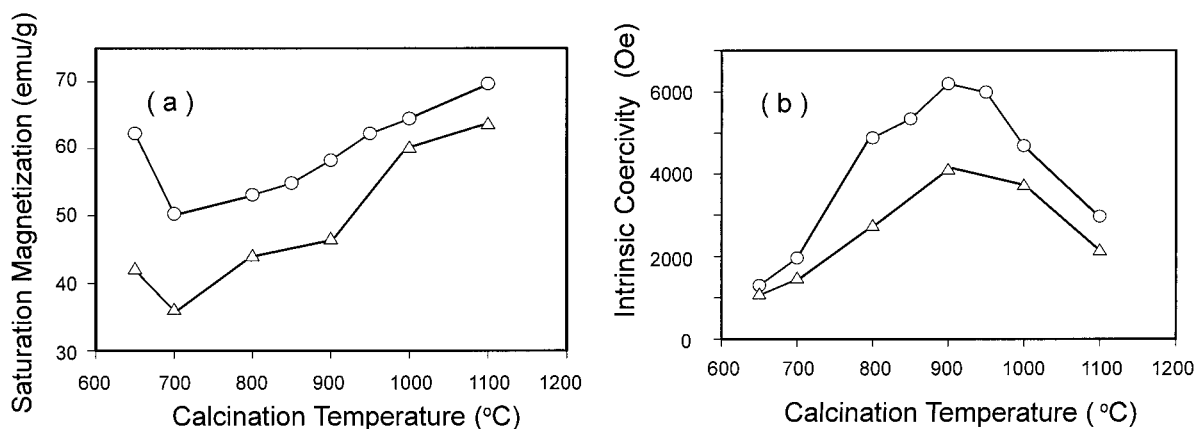


Fig. 12. (a) Saturation magnetization and (b) intrinsic coercivity, as a function of the calcination temperature ((○) powder derived from ethanol-based microemulsion and (△) conventionally coprecipitated powder).

Acknowledgments

The authors wish to thank Miss Chai Hoon Quek and Ms. Xianzhen Wang for their kind assistance in XRD and magnetic measurement, respectively.

References

- ¹H. Kojima, "Fundamental Properties of Hexagonal Ferrites with Magnetoplumbite Structure"; Ch. 5, pp. 305–91 in *Ferromagnetic Materials: A Handbook on the Properties of Magnetically Ordered Substances*, Vol. 3. Edited by E. P. Wohlfarth. North-Holland Publishing, Amsterdam, The Netherlands, 1982.
- ²P. Hernández, C. de Francisco, J. M. Muñoz, J. Iniguez, L. Torres, and M. Zazo, "Influence of Sintering Atmosphere on the Magnetic Aftereffect in Strontium Ferrites," *J. Magn. Magn. Mater.*, **157/158**, 123–24 (1996).
- ³H. Stäblein, "Hard Ferrites and Plastoferrites"; see Ref. 1, Ch. 7, pp. 441–602.
- ⁴H. Kojima; see Ref. 1, pp. 307–66.
- ⁵F. Habery and A. Kockel, "The Formation of Strontium Hexaferrite SrFe₁₂O₁₉ from Pure Iron Oxide and Strontium Carbonate," *IEEE Trans. Magn.*, **Mag-12**, 983–85 (1976).
- ⁶S. Blackburn, T. P. Johnson, C. B. Ponton, and M. H. L. Wise, "Ceramic and Metals Development—A Selective Overview"; pp. 771–81 in *Chemical Engineering Research & Design—Transactions of The Institution of Chemical Engineers, Part A*, Vol. 73. Institution of Chemical Engineers, Warwickshire, U.K., 1995.
- ⁷E. P. Wohlfarth; see Ref. 1, pp. 334–42.
- ⁸Z. Jin, W. Tang, J. Zhang, H. Lin, and Y. Du, "Magnetic Properties of Isotropic SrFe₁₂O₁₉ Fine Particles Prepared by Mechanical Alloying," *J. Magn. Magn. Mater.*, **182**, 231–37 (1993).
- ⁹V. V. Pankov, M. Pernet, P. Germi, and P. Mollard, "Fine Hexaferrite Particles for Perpendicular Recording Prepared by the Coprecipitation Method in the Presence of an Inert Component," *J. Magn. Magn. Mater.*, **120**, 69–72 (1993).
- ¹⁰S. Kulkarni, J. Shrotri, C. E. Deshpande, and S. K. Date, "Synthesis of Chemically Coprecipitated Hexagonal Strontium Ferrite and Its Characterization," *J. Mater. Sci.*, **24**, 3739–44 (1989).
- ¹¹S. E. Jacobo, C. Domingo-Pascual, R. Rodriguez-Clemente, and M. A. Blesa, "Synthesis of Ultrafine Particles of Barium Ferrite by Chemical Coprecipitation," *J. Mater. Sci.*, **32**, 1025–28 (1997).
- ¹²W. Roos, "Formation of Chemically Coprecipitated Barium Ferrite," *J. Am. Ceram. Soc.*, **63** [11–12] 601–603 (1980).
- ¹³K. Haneda, C. Miyakawa, and K. Goto, "Preparation of Small Particles of SrFe₁₂O₁₉ with High Coercivity by Hydrolysis of Metal-organic Complexes," *IEEE Trans. Magn.*, **Mag-23**, 3134–36 (1987).
- ¹⁴J.-H. Choy, Y.-S. Han, and S.-W. Song, "Preparation and Magnetic Properties of Ultrafine SrFe₁₂O₁₉ Particles Derived from a Metal Citrate Complex," *Mater. Lett.*, **19**, 257–62 (1994).
- ¹⁵C. Stürig, K. A. Hempel, and D. Bonnenberg, "Formation and Microwave Absorption of Barium and Strontium Ferrite Prepared by Sol-Gel Technique," *Appl. Phys. Lett.*, **63**, 2836–38 (1993).
- ¹⁶R. Ardiaca, R. Ramos, A. Isalgué, J. Rodriguez, X. Obradors, M. Pernet, and M. Vallet, "Hexagonal Ferrite Particles for Perpendicular Recording Prepared by the Precursor Method," *IEEE Trans. Magn.*, **Mag-23**, 22–24 (1987).
- ¹⁷Y. Senzaki, J. Caruso, M. J. Hampden-Smith, T. T. Kodas, and L.-M. Wang, "Preparation of Strontium Ferrite Particles by Spray Pyrolysis," *J. Am. Ceram. Soc.*, **78** [11] 2973–76 (1995).
- ¹⁸H. Sato and T. Umeda, "Grain Growth of Strontium Ferrite Crystallized from Amorphous Phases," *Mater. Trans., JIM*, **34** [1] 76–81 (1993).
- ¹⁹D. Bahadur and D. Chakravorty; see Ref. 11, pp. 189–93.
- ²⁰K. Oda, T. Yoshio, K. O. Oka, and F. Kanamaru, "Magnetic Properties of SrFe₁₂O₁₉ Particles Prepared by the Glass-Ceramic Method," *J. Mater. Sci. Lett.*, **3**, 1007–10 (1984).
- ²¹O. Kubo, T. Ido, and H. Yokoyama, "Properties of Barium Ferrite Particles for Perpendicular Magnetic Recording Media," *IEEE Trans. Magn.*, **Mag-18** [6] 1122–24 (1982).
- ²²J. H. Lee, H. S. Kim, and C. W. Won, "Magnetic Properties of Strontium Ferrite Powder Made by Hydrothermal Processing," *J. Mater. Sci. Lett.*, **15**, 295–97 (1996).
- ²³A. Ataie, I. R. Harris, and C. B. Ponton, "Magnetic Properties of Hydrothermally Synthesized Strontium Hexaferrite as a Function of Synthesis Conditions," *J. Mater. Sci.*, **30**, 1429–33 (1995).
- ²⁴C. H. Lin, Z. W. Shih, T. S. Chin, M. L. Wang, and Y. C. Yu, "Hydrothermal Processing to Produce Magnetic Particles," *IEEE Trans. Magn.*, **Mag-26** [1] 15–17 (1990).
- ²⁵A. Ataie, I. R. Harris, and C. B. Ponton, "Hydrothermal Synthesis of Strontium Hexaferrite: Powder Composition, Morphology, and Magnetic Properties"; pp. 273–81 in *Introduction to Magnetism and Magnetic Materials*. Edited by J. David. Chapman and Hall, London, U.K., 1991.
- ²⁶J. Fang, J. Wang, S.-C. Ng, C.-H. Chew, and L.-M. Gan, "Ultrafine Zirconia Powders via Microemulsion Processing Route," *Nanostruct. Mater.*, **8**, 499–505 (1997).
- ²⁷P. Vaqueiro, M. A. López-Quintela, and J. Rivas, "Synthesis of Yttrium Iron Garnet Nanoparticles via Coprecipitation in Microemulsion," *J. Mater. Chem.*, **7**, 501–504 (1997).
- ²⁸V. Chhabra, M. Lal, and A. N. Maitra, "Nanophase BaFe₁₂O₁₉ Synthesized from a Nonaqueous Microemulsion with Ba- and Fe-containing Surfactants," *J. Mater. Res.*, **10**, 2689–92 (1995).
- ²⁹M. A. López-Quintela and J. Rivas, "Chemical Reactions in Microemulsions: A Powerful Method to Obtain Ultrafine Particles," *J. Colloid Interface Sci.*, **158**, 446–51 (1993).
- ³⁰L. M. Gan, L. H. Zhang, H. S. O. Chan, C. H. Chew, and B. H. Loo, "A Novel Method for the Synthesis of Perovskite-Type Mixed Metal Oxides by the Inverse Microemulsion Technique," *J. Mater. Sci.*, **31**, 1071–79 (1996).
- ³¹(a)I. Rico and A. Lattes, "A New Type of Water-Insoluble Surfactants and Nonaqueous Microemulsions—Formamide as a Water Substitute IX: Waterless Microemulsions 6"; Ch. 23, pp. 357–75 in *Microemulsion Systems*. Edited by H. L. Rosano and M. Clause. Marcel Dekker, New York, 1987. (b)"A Study of Cyclocondensation Reactions in Waterless Microemulsions—Formamide as a Water Substitute X: Waterless Microemulsions 7"; *ibid.*, Ch. 24, pp. 377–85.
- ³²K. V. Schubert, K. M. Lusvardi, and E. W. Kaler, "Polymerization in Nonaqueous Microemulsions," *Colloid Polym. Sci.*, **274**, 875–83 (1996).
- ³³(a)C. J. Pouchert (Ed.), *The Aldrich Library of FT-IR Spectra*, Vol. 1. Aldrich Chemical Co., Inc., Milwaukee, WI, 1985. (b)R. J. Keller (Ed.), *The Sigma Library of FT-IR Spectra*, Vol. 2. Sigma Aldrich Corp., St. Louis, MO, 1986. (c)C. J. Pouchert (Ed.), *The Aldrich Library of Infrared Spectra*, 3rd ed. Aldrich Chemical Co., Inc., 1981.
- ³⁴G. Socrates (Ed.), *Infrared Characteristic Group Frequencies*, 2nd ed. Wiley, Chichester, U.K., 1994.
- ³⁵K. Nakamoto, "Part II. Inorganic Compounds"; p. 106 in *Infrared and Raman Spectra of Inorganic and Coordination Compounds*, 4th ed. Wiley-Interscience, New York, 1986.
- ³⁶R. A. Nyquist and R. O. Kagel (Eds.), *Infrared Spectra of Inorganic Compounds*, Vol. 4. Academic Press, San Diego, CA, 1997.
- ³⁷X. Li, G. Lu, and S. Li, "Synthesis and Properties of Strontium Ferrite Ultrafine Powders," *J. Mater. Sci. Lett.*, **15**, 397–99 (1996).
- ³⁸G. Bate, "Oxide for Magnetic Recording"; Ch. 12, pp. 711–13 in *Magnetic Oxides, Part 2*. Edited by D. J. Craik. Wiley-Interscience, London, U.K., 1975.
- ³⁹R. Nawathey-Dikshit, S. R. Shinde, S. B. Ogale, S. D. Kulkarni, S. R. Sainkar, and S. K. Date, "Synthesis of Single-Domain Strontium Ferrite Powder by Pulsed Laser Ablation," *Appl. Phys. Lett.*, **68**, 3491–93 (1996).
- ⁴⁰R. Valenzuela, *Magnetic Ceramics*. Cambridge University Press, Cambridge, U.K., 1994. □